京都大学学術情報リポジトリ
KURENAI 紅
Kyoto University Research Information Repository

京都大学
KYOTO UNIVERSITY

Title	Decrease in topoisomerase I is responsible for activation-induced cytidine deaminase (AID)-dependent somatic hypermutation.
Author(s)	Kobayashi, Maki; Sabouri, Zahra; Sabouri, Somayeh; Kitawaki, Yoko; Pommier, Yves; Abe, Takaya; Kiyonari, Hiroshi; Honjo, Tasuku
Citation	Proceedings of the National Academy of Sciences of the United States of America (2011), 108(48): 19305-19310
Issue Date	2011-11-29
URL	http://hdl.handle.net/2433/152359
Right	©2012 by the National Academy of Sciences
Type	Journal Article
Textversion	author

Kyoto University

Classification: BIOLOGICAL SCIENCES, Genetics.

Decrease in topoisomerase I is responsible for AID-dependent somatic hypermutation

Maki Kobayashi, Zahra Sabouri, Somayeh Sabouri, Yoko Kitawaki, Yves Pommier[*], Takaya Abe[†], Hiroshi Kiyonari[†], and Tasuku Honjo[1]

Department of Immunology and Genomic Medicine, Graduate School of Medicine, Kyoto University, Yoshida Sakyo-ku, Kyoto 606-8501, Japan.

[*]Laboratory of Molecular Pharmacology, Center for Cancer Research, National Cancer Institute, NIH, Bethesda, MD 20892-4255, USA.

[†]Laboratory for Animal Resources and Genetic Engineering, RIKEN Center for Developmental Biology, 2-2-3 Minatojima Minami, Chuou-ku, Kobe 650-0047, Japan

Corresponding author: Tasuku Honjo; Phone +81-75-753-4371; Fax +81-75-753-4388; E-mail honjo@mfour.med.kyoto-u.ac.jp

Abstract

Somatic hypermutation (SHM) and class-switch recombination (CSR) of the immunoglobulin gene require both transcription of the locus and the expression of activation-induced cytidine deaminase (AID). During CSR, AID decreases the amount of topoisomerase I (Top1); this decrease alters the DNA structure and induces cleavage in S region. Similarly, Top1 is involved in transcription-associated mutation (TAM) at dinucleotide repeat in yeast and in triplet repeat contraction in mammals. Here, we report that the AID-induced decrease in Top1 is critical for SHM. Top1 knockdown or haploinsufficiency enhanced SHM, whereas Top1 overexpression down-regulated it. A specific Top1 inhibitor, camptothecin, suppressed SHM, indicating that Top1's activity is required for DNA cleavage. Nonetheless, suppression of transcription abolished SHM, even in cells with Top1 knockdown, suggesting that transcription is critical. These results are consistent with a model proposed for CSR and triplet instability, in which transcription-induced non-B structure formation is enhanced by Top1 reduction, and provides the target for irreversible cleavage by Top1. We speculate that the mechanism for transcription-coupled genome instability was adopted to generate immune diversity when AID evolved.

¥body

Introduction

The immunoglobulin (Ig) locus undergoes two types of genetic alteration, somatic hypermutation (SHM) and class switch recombination (CSR), to generate antibody memory against given antigens when B lymphocytes are stimulated by pathogens. Both SHM and CSR depend on the expression of activation-induced cytidine deaminase (AID) (1, 2) and transcription of the target Ig loci (3-6).

AID is responsible for introducing DNA cleavage in the variable (V) region and the switch (S) region of the Ig locus for initiating SHM and CSR, respectively (7-10). AID's DNA cleavage activity is associated with its amino-terminal region, because mutations at the carboxyl (C)-terminus abolish CSR without affecting SHM and DNA cleavage in the S region (7, 11, 12). It is likely that the C-terminal region of AID is required for the recombination of the cleaved S region ends. Thus, AID carries out two separate functions with a single catalytic center located in the middle of the protein. Under normal conditions, AID is only expressed in activated B cells and introduces genetic alterations in the Ig gene. However, Ig genes are not the only targets of AID (13, 14). Indeed, AID is involved in *Ig-c-myc* chromosomal translocation, causing malignant tumors (15, 16). More recently, certain pathogens were reported to induce the activation of AID, which may cause tumorigenesis over the long-term (17-20).

Using an artificial construct to monitor CSR and SHM, positive correlations between transcription levels and the efficiencies of CSR and SHM have been demonstrated (21, 22). Transcription-associated genomic instability has been extensively studied in a number of systems (23). One finding of these studies is that the frequency of mutations, including base replacements and deletions, caused by transcription-associated mutagenesis (TAM) increased in parallel with the

transcription enhancement of the specific loci. Recently, 2-5-base deletions by TAM in two different loci in yeast, *Can1* and *Lys2*, were shown to depend on topoisomerase I (Top1) (24, 25). In the absence of Top1, TAM was decreased, drastically affecting deletions, with less effect on the number of base replacements. The deletion of 2-5 bases takes place frequently at hot spots that contain dinucleotide (AT) repeats. Transcription is also required for the contraction or expansion of triplet repeats; these changes are associated with human diseases, including Huntington's disease, myotonic dystrophy type 1, and spinocerebellar ataxia (26). Triplet repeats are believed to form non-B structures caused by the excessive negative superhelicity induced by active transcription. A recent report provided evidence that Top1 introduces irreversible cleavage at triplet repeats in a transcription-dependent manner (27).

Normally, Top1 corrects the transcription-induced excessive supercoiling by nicking, covalently binding to DNA through phospho-tyrosine bond, rotating DNA along the helix, and finally religating the nicked end (28). When the transcription rate exceeds the capacity of Top1, excessive negative supercoiling accumulates at the rear of the transcription machinery, increasing the chance of non-B structure formation at repeat or palindrome-rich regions (29). Top1 cuts non-B DNA and forms a DNA-bound intermediate, but cannot rotate around the helix, resulting in irreversible cleavage and mutagenesis (27). Thus, the appropriate balance between the transcription rate and Top1 activity appears to be critical for maintaining genome stability. In agreement with this assumption, a decrease in Top1 in mammalian cells induces genome instability (30, 31).

We recently showed that AID reduces the protein level of Top1, which induces CSR (32). Furthermore, we showed that artificially reduced levels of Top1 also enhance CSR in CH12F3-2A B lymphoma cells and splenic B cells. This effect is associated with increased DNA cleavage in the S

region. In addition, camptothecin (CPT), a specific inhibitor of Top1 catalytic activity, blocks DNA breaks and CSR without affecting transcription of the S region.

Here we report that AID decreases the level of Top1 in SHM-proficient cells and that further reduction of the Top1 protein level by knockdown or haploinsufficiency augments SHM. By contrast, the overexpression of Top1 down-regulated SHM frequency. Furthermore, a concurrent, gradual decrease in the transcription of the target locus reduced SHM efficiency, regardless of Top1 knockdown. Finally, SHM efficiency was inhibited by a low dose of CPT. These results collectively indicate that the AID-induced genetic alterations CSR and SHM share, at least in part, the Top1-mediated DNA cleavage mechanism of TAM at dinucleotide repeat hot spots and triplet repeat contraction.

Results

Decrease in Top1 increases the frequency of SHM in B cells

Previously, we showed that AID decreases the Top1 level in CH12F3-2A cells, which undergo CSR but not SHM (32). To confirm the AID-induced reduction of Top1 in SHM-proficient cells, we used AID-knockout BL2 cells (human Burkitt's lymphoma line) (33) that express a fusion protein of AID and the estrogen receptor (ER) binding domain (BL2-AID$^{-/-}$AIDER). As expected, the amount of Top1 clearly decreased, by about half in the BL2-AID$^{-/-}$ AIDER cells, 6 hours after stimulation with 4-OHT (Fig. 1A). AIDER activation simultaneously caused the accumulation of SHM (Table 1A-B).

We next examined the effect of Top1 knockdown on SHM by transfecting an siRNA oligo that suppresses hTop1 (hTop1#3) or control oligos with the same GC content. The Top1 level was efficiently suppressed by the siRNA (Fig. 1B), and accompanied by an increase in SHM frequency in the expressed V (V_H4-39-J_H5) gene sequence (33) (Table 1A). However, the difference between the Top1-knockdown and the control samples was not large enough to demonstrate statistical significance. The base substitution pattern of the Top1-knockdown sample was similar to that of the control. The base substitution profiles were stable throughout the mutation analyses in the present study (Supplementary Table 1). Since the SHM augmentation by Top1 knockdown was not statistically significant in the V region, we examined the SHM frequency of the Sμ region because the mutation frequency in this region is AID-dependent and generally higher than in the V region (9). In the Sμ region, the SHM frequency was significantly increased by Top1 knockdown compared with the control oligo-transfected sample (Table 1B).

To examine the effect of Top1 reduction on SHM *in vivo*, we generated a Top1 conditional knockout mouse with a floxed *exon 15* (*Top1*^{f}), which is detected as a 6.2-kb HindIII fragment by the 3' Probe A (Fig. 1C-D). Top1 heterozygotes (*Top1*$^{-/+}$) were generated by crossing *Top1*$^{f/+}$ mice with *CAG-Cre* transgenic mice. Although the *exon 15* deletion should produce a shorter Top1 protein, the

heterozygotes contained half the amount of Top1 as wild type (WT), probably due to instability of the mutant mRNA or protein (Fig. 1E). We next examined the effect of the Top1 haploinsufficiency on SHM *in vivo*. Germinal center B cells were isolated from the Peyer's patches of heterozygotes and WT littermates, and their genomic DNA was extracted for SHM analysis. The SHM frequency at the V_HJ558-J_H4 region was about 2-fold higher in the Top1 heterozygotes than in the WT littermates, with high statistical significance (Table 1C). These results clearly indicate that the Top1 reduction enhances SHM. Note that the mutation frequency of the Top1-decreased BL2 cells was similar to that of control oligo-transfected cells without AID activation (Table 1A-B), indicating that the Top1 reduction alone does not induce SHM.

Top1 over-expression suppresses SHM

To further confirm Top1's involvement in SHM, we used a Top1-deficient P388/CPT45 subline, which was previously established from the mouse B-cell lymphocytic leukemia line P388, by selection in the presence of 45 μM CPT (34, 35). The P388/CPT45 cells actually expressed an extremely low level of Top1 of the normal size (Fig. 2A, arrow 1) and a low amount of aberrant Top1 of about 135 kDa (Fig. 2A, arrow 2), indicating that the P388/CPT45 cells were Top1 insufficient but not completely deficient. P388 cells contain rearranged forms of the Ig κ-chain and heavy-chain loci, but do not express Ig on their surface, which we confirmed by RT-PCR and surface staining (36). Nonetheless, the expression level of μ-germline transcripts from the Iμ promoter was comparable among the P388, P388/CPT45, and CH12F3-2A cells (Fig. 2B). It is therefore likely that exogenous AID expression induces SHM in the 5'-flanking region of the Sμ core sequence, although P388 and P388/CPT45 cells do not express endogenous AID (Fig. 2A, arrow 4). AIDER was retrovirally introduced into both the parental P388 and the P388/CPT45 cells (Fig. 2A, arrow 5). When AIDER was activated by adding 4-OHT, the SHM frequency was significantly higher in the

P388/CPT45-AIDER cells (2.56 x 10^{-4}) than in the P388-AIDER cells (0.71 x 10^{-4}), in agreement with the above observations that the Top1 reduction enhances SHM (Table 2A).

To further confirm the critical role of the Top1 protein level in determining the SHM frequency, GFP-fused human Top1 (GFP-hTop1) was introduced into the Top1-insufficient P388/CPT45-AIDER cells (Fig. 2A, arrow 3). The expression level of GFP-hTop1 in the P388/CPT45-AIDER cells was much higher than their endogenous Top1, and was similar to that of Top1 in the parental P388-AIDER cells. The SHM frequency in the Sμ region was drastically reduced (2.2 x 10^{-4}) in the GFP-hTop1-supplemented P388/CPT45-AIDER cells compared to the control GFP-transfected P388/CPT45-AIDER cells (6.3 x 10^{-4}) (Table 2B). Although hTop1 supplementation in the P388/CPT45-AIDER cells reduced the SHM frequency, the cell proliferation rate was hardly affected, suggesting that the reduction in SHM frequency was not due to a change in the cell-proliferation rate (Fig. 2C).

SHM augmentation by Top1 reduction depends on transcription

Since transcription of the target locus is required for SHM and the efficiency of transcription correlates with SHM frequency, it was important to examine whether the Top1 reduction-associated SHM augmentation was dependent on transcription. For this purpose, we used NTZ cells, which is NIH3T3 cells carrying the construct "pI", tetracycline(*tet*)-repressible GFP with a premature stop codon (22). An AIDER transfectant of NTZ (Figure 3A) accumulates reversion mutations at the stop codon in GFP upon 4-OHT addition, and allows quick SHM detection by GFP reversion expression (37).

To confirm that the Top1 reduction increases SHM even in non-B cells, NTZ-AIDER fibroblast cells were transfected with Top1 siRNA oligos (mTop1#35 and #97) or a control oligo sequence, followed by stimulation with 4-OHT. AIDER activation by 4-OHT induced a decrease in

Top1 in NTZ cells, and the Top1 protein expression was further reduced by the two siTop1 oligos (Fig. 3B). The GFP reversion frequency increased from 0.84% in the control to 1.08% (mTop1 #35) or 1.22% (mTop1 #97) (Fig.3C), whereas the 4-OHT non-stimulated samples had a very low GFP expression frequency (0.07-0.19%). Consistent with these findings, Top1 knockdown increased the SHM frequency, as assessed by a sequence comparison of the GFP gene, from 2.9×10^{-3} (control) to 4.5×10^{-3} (mTop1#35) or 4.7×10^{-3} (mTop1#97) (Table 3). The difference was highly statistically significant.

The NTZ-AIDER system allows the transcriptional activity of the SHM target GFP to be modulated by the titration of *tet*. To test whether transcription of the target was dominant over the Top1 reduction for SHM, the GFP reversion was examined in NTZ-AIDER cells with Top1 knockdown in the presence of serially diluted concentrations of *tet* (Fig. 3D). NTZ-AIDER cells treated with mTop1#35 or mTop1#97 showed approximately doubled rates of GFP reversion (0.9 and 0.95%) compared with the control (0.55%) in the absence of *tet,* while the GFP reversion gradually declined, reaching almost zero at 50 ng/ml *tet,* regardless of the Top1 knockdown. These results clearly indicate that transcription has the dominant effect in SHM, which is also true for TAM, CAG-repeat deletion, and CSR (21, 24, 25, 27).

Top1 activity required for SHM in fibroblasts and B cells

We next examined the requirement of Top1 activity for SHM. The complete deletion of Top1 in mammals is lethal at the pre-implantation stage (38). We therefore investigated the effect of CPT on SHM in NTZ-AIDER cells. The addition of 30 nM CPT strongly inhibited the GFP reversion induced by 4-OHT in the NTZ-AIDER cells (Fig. 4A). The DNA sequence determination of the GFP-coding region confirmed that the mutation frequency was indeed reduced by the addition of 30 nM CPT, to less than one-fourth its level without CPT (6.1×10^{-4} vs. 1.5×10^{-4}) (Table 4A). This SHM reduction

was not due to cell death or the inhibition of target transcription, because 96 and 98% of the 30 nM CPT-treated and non-treated cells, respectively, remained alive (Fig. 4B), and transcription of the target GFP was not changed by the 30 nM CPT treatment (Fig. 4C).

To confirm the inhibitory effect of CPT on the SHM in B cells, we established a sensitive SHM assay in B cells to avoid the side effects of CPT during long-term incubation. First, we expressed a C-terminally truncated form of AID (JP8Bdel) fused with ER in BL2 cells, because JP8Bdel has 4-fold stronger DNA-cleavage activity and SHM efficiency than WT AID (7). In fact, stimulation of the BL2 cells expressing JP8BdelER (BL2-JP8BdelER) with 1 μM 4-OHT for 3 hours decreased the Top1 protein amount to about a half of the control level (Fig. 4D), which is much faster than the rate obtained with AIDER (Fig. 1A). Second, we chose the S region as the target, because it is 5 times more frequently mutated than the V region (7). Using this system, we observed 7.2×10^{-4} mutations in the 5'-flanking region of the Sμ region 24 hours after the addition of 4-OHT, while endogenous WT AID in BL2 cells induced only 1.7×10^{-4} mutations (Table 4B). When 30 nM CPT was added to the culture one hour before the activation of JP8BdelER by 4-OHT, the SHM frequency was reduced to 3.5×10^{-4}, although some cell death was induced in the BL2 cells (20% at 30 nM CPT). Since CPT drastically reduced the SHM in two different systems, we conclude that Top1 activity is required for SHM, as for the base deletion by TAM and the DNA cleavage in CSR.

Discussion

Involvement of Top1 in SHM

In the present study, we showed that the AID-dependent decrease in Top1 induces SHM, and that additional Top1 knockdown augments SHM further, as previously shown for CSR (32). By contrast, Top1 over-expression suppresses the AID-dependent SHM. SHM frequency is thus inversely correlated with Top1 level. SHM also depends on the catalytic activity of Top1, because CPT drastically reduced SHM. From these lines of evidence, Top1 itself may make an irreversible cleavage at the transcription-associated non-B DNA structures in the V region, whose formation is enhanced by the partial Top1 deficiency. Moreover, the SHM efficiency quantitatively correlates with both the target's transcription level (22) and the Top1 reduction by knockdown. Thus, transcription enhancement and Top1 reduction have the same augmenting effect on the accumulation of the DNA superhelicity, which enhances the non-B structure formation.

Transcription-induced non-B structure formation

Transcription is by its nature dangerous to the maintenance of genome integrity (23). In eukaryotes, transcription requires disassembly of the tightly packed chromatin structure and chromatin reassembly (39), accompanied by the exposure of naked DNA and R-loop formation (40). Furthermore, during transcription, a local distortion of the DNA superhelix is created, positive in the front and negative in the rear of the transcription machinery (41), that enhances the non-B structure formation (42).

Because of these effects, excessive transcription is associated with mutations, deletions, recombination, and other genetic events. The transcription-induced non-B DNA structure formed at repetitive or palindromic sequences is considered the major risk for genetic instability (41, 43). A model linking transcription and non-B structures has been proposed for triplet repeat contraction/expansion, which is associated with human diseases such as Huntington's disease (26). Dinucleotide repeat sequences are hot spots for deletions and mutations in TAM (24, 25). The

transcription of target loci is also required for physiological recombination and mutational events, such as meiotic recombination, VDJ recombination, CSR, and SHM, although not all of these event may require the non-B structure formation (4, 21, 44, 45).

Top1 reduction augments the non-B structure formation and causes irreversible cleavage

Since Top1 regulates the DNA superhelical density at the transcription sites, it is reasonable to suppose that transcription-induced non-B structure formation is enhanced by Top1 reduction. Gangloff et al (46) showed that the loss of Top1 increases genetic instability in yeast and suggested that CSR may depend on transcription-induced non-B configuration in the repetitive sequences of the Sα region during CSR. Recently, Top1 was also shown to be involved in the transcription-induced triplet repeat deletion in mammals (27). Top1 knockdown causes an increase in triplet contraction, In addition, suppression of the enzymes which remove DNA-bound Top1 also enhances triplet contraction. The results suggest that Top1 may cut non-B structures but cannot rotate around the helix, which results in irreversible cleavage. Furthermore, recent reports about TAM in yeast have shown that the 2-5-base deletion at dinucleotide repeats is almost completely dependent on the catalytic activity of Top1 (24, 25). Chromatin immunoprecipitation without crosslinking reagent demonstrated that Top1 is covalently binding to the target gene in a transcription-dependent manner, suggesting that Top1 is responsible for the DNA cleavage in TAM. These results are consistent with the observation that Top1 reduction causes genetic instability in mammalian cells. The long-term culture of P388/CPT45 cells carrying a low level of Top1 causes the accumulation of γH2AX focus formation on various chromosomes (31). Extensive chromosomal translocation is also observed in this cell line. We showed that AID reduces Top1, to initiate CSR. Since the S region consists of repetitive and palindromic sequences, the transcription–induced excessive negative superhelix induces non-B structures, leading to irreversible cleavage by Top1 (32).

Target determination of SHM

Triplet contraction in mammalian cells and TAM in yeast may depend on non-B structure-associated irreversible cleavage by Top1, because deletions take place in regions of triplet repeats and dinucleotide repeat hotspots, respectively. The S region also contains many repeats that appear to form non-B structures. Although the V region does not contain many repeated sequences, a computer analysis indicated that the V region can form non-B-type structures, especially stem-loops, under excessively negative supercoiled conditions (47, 48). The GFP sequence can also form stem-loop structures (http://mfold.rna.albany.edu/?q=DINAMelt/Quickfold).

Although AID targets are not absolutely limited to Ig loci, they are not random, because there are several preferred mutated loci in the genome (13, 14). Non-B DNA structure formation may be required for the DNA cleavage in SHM. However, it may not be sufficient to explain all the DNA-cleavage loci targeted by AID, because not all repetitive sequences seem to accumulate mutations after AID activation *in vivo*. AID targets appear to be determined by a combination of *cis* (DNA structure) and *trans* (DNA-binding proteins) factors. We previously showed that histone modification H3K4 trimethylation in the S region is essential for DNA cleavage in CSR (49). H3K4 trimethylation is an important marker for meiotic recombination and VDJ recombination (50, 51). Thus, it will be important to examine whether other AID target loci have non-B-prone sequences or not. It will also be interesting to investigate whether H3K4 trimethylation is required for SHM.

Evolution of adaptive immunity

SHM, CSR, TAM, and triplet repeat contraction may all share a DNA-cleavage mechanism: (a) non-B structure formation regulated by the Top1 protein level and the locus transcription level and (b) irreversible cleavage by Top1. Thus, AID probably adopted the basic mechanism of transcription-coupled genome instability to make DNA cleavage in immunoglobulin locus, when adaptive immunity evolved in vertebrates. Such an evolutionary origin makes it inevitable that AID targets are not absolutely specific to Ig loci. However, the subsequent processes for inducing SHM and CSR appear to be different from those of TAM with dinucleotide repeat hot

spots and triplet repeat expansion/contraction. For example, triplet contraction/expansion does not appear to be AID-dependent. It is notable that Top1 reduction alone does not cause SHM unless AID is activated. Since we assume that AID edits a microRNA to reduce the translation of Top1 mRNA, the edited miRNA may activate another functional protein necessary for the DNA cleavage or repair step in SHM (32).

Materials and Methods

Cells and reagents

BL2-AID$^{-/-}$ AIDER cells were generated by transfecting the human Burkitt's lymphoma-derived BL2 cell subclone, BL2-AID$^{-/-}$ (33) with AIDER (52). BL2-JP8BdelER was generated by transfecting BL2 cells with JP8BdelER (7). NTZ cells (37) were infected with an AID-ER-expressing retrovirus to generate NTZ-AIDER cells. P388 and P388/CPT45 cells (35) were infected with pFB-AIDER-IRES-puro for SHM analysis. P388/CPT45-AIDER was transfected with linearized EF-EGFP or EF-EGFP-hTop1 plasmid by electroporation, selected with G418 for 6 days, and sorted by GFP fluorescence with a FACS ARIA-II (BD). CPT was purchased from Calbiochem and dissolved in dimethylsulfoxide (DMSO).

Human Top1 expression vecto

The EGFP gene (Clontech) was fused to the N-terminus of the human Top1 (hTop1) coding region in the pBlueScript vector (Promega). The EGFP-hTop1 cassette was then inserted between the SmaI-XbaI sites of pEF-BOS (53). As the control, EGFP alone was also cloned into pEF-BOS.

Top1 knockdown

For the knockdown of Top1 in BL2-AID$^{-/-}$AIDER cells, the Stealth siRNA oligo hTop1#3 (HSS110895, Invitrogen) was electroporated by the Nucleofector ™ 96-well Shuttle™ system (Lonza). To achieve the knockdown in NTZ-AIDER cells, mTop1#35 (Top1-MSS212035) and mTop1#97 (MSS278497) were transfected into the cells using the Lipofectamine™ RNAiMAX Transfection Reagent (Invitrogen) following the manufacturer's instructions. Stealth RNAi Negative Control Low or Med GC (Invitrogen) was used as a control. All the sequences of the siRNA oligos are shown in Supplementary Table 2A.

Top1 knockout mouse

The conditional knockout mice (RIKEN Accession number CDB0799K:

http://www.cdb.riken.jp/arg/mutant%20mice%20list.html) with a floxed *exon 15* of the *Top1* locus were generated by the Laboratory for Animal Resources and Genetic Engineering, RIKEN, Center for Developmental Biology (Kobe, Japan), and maintained and used at the Institute of Laboratory Animals, Graduate School of Medicine, Kyoto University, according to approved protocols for animal experiments. The genotype of the floxed allele was confirmed by Southern blotting using Probe A, amplified with the primers 3'Probe-F and 3'Probe-R. Heterozygotes of the Top1 floxed allele with the neomycin-resistance gene ($Top1^{fl/+}$) were crossed with CAG-Cre mice to obtain the *exon 15*-deleted allele ($Top1^{-/+}$). The CAG-Cre mice (B6.Cg-Tg(CAG-Cre)CZ-MO2Osb, produced by Dr. Masaru Okabe, Osaka University, Japan) were provided by the RIKEN BRC through the National Bio-Resource Project of the MEXT, Japan. Wild-type C57BL/6 mice were purchased from CLEA Japan. Genotypes of the compound mice were determined by genomic PCR with KOD FX (TOYOBO). The germinal center B cells from the Peyer's patches of 16- to 25-week-old mice were sorted by FACS Aria II after staining with a mixture of FITC-labeled PNA (Vector Laboratories), CD95-APC (e-Bioscience), and B220-PE (e-Bioscience). The PNA^+B220^+ population was sorted from mice of litter #1, and the $PNA^+CD95^+B220^+$ population was recovered from those of litters #2 and #3.

Other methods

To analyze the SHM frequency, KOD Plus Neo (TOYOBO), Pyrobest (TaKaRa), or PrimeStar (TaKaRa) was used to amplify the regions. The obtained PCR fragments were cloned into the pGEM-T easy vector (Promega) or pBlueScript (Stratagene). The BigDye (ABI) cycle sequencing kit and ABI7700 genetic analyzer were used for sequencing. Viral infection, Western blotting, measurement of Western blotting signals, and quantitative RT-PCR were performed as previously described (32). The primer sequences for cloning or genotyping and the antibodies used in Western blotting are listed in Supplementary Table 2.

Acknowledgement

The authors are grateful to Dr. Kei-ichiro Suzuki for the method of the germinal center B-cell isolation, and to Ms. Y. Shiraki for preparation of the manuscript. This research was supported by a Grant-in-Aid for Specially Promoted Research 17002015 of the Ministry of Education, Culture, Sports, Science and Technology of Japan.

References

1. Muramatsu M*, et al.* (2000) Class switch recombination and hypermutation require activation-induced cytidine deaminase (AID), a potential RNA editing enzyme. *Cell* 102(5):553-563.
2. Revy P*, et al.* (2000) Activation-induced cytidine deaminase (AID) deficiency causes the autosomal recessive form of the Hyper-IgM syndrome (HIGM2). *Cell* 102(5):565-575.
3. Yancopoulos GD*, et al.* (1986) Secondary genomic rearrangement events in pre-B cells: V_HDJ_H replacement by a LINE-1 sequence and directed class switching. *Embo J* 5(12):3259-3266.
4. Fukita Y, Jacobs H, & Rajewsky K (1998) Somatic hypermutation in the heavy chain locus correlates with transcription. *Immunity* 9(1):105-114.
5. Peters A & Storb U (1996) Somatic hypermutation of immunoglobulin genes is linked to transcription initiation. *Immunity* 4(1):57-65.
6. Stavnezer-Nordgren J & Sirlin S (1986) Specificity of immunoglobulin heavy chain switch correlates with activity of germline heavy chain genes prior to switching. *Embo J* 5(1):95-102.
7. Doi T*, et al.* (2009) The C-terminal region of activation-induced cytidine deaminase is responsible for a recombination function other than DNA cleavage in class switch recombination. *Proc Natl Acad Sci U S A* 106(8):2758-2763.
8. Petersen S*, et al.* (2001) AID is required to initiate Nbs1/gamma-H2AX focus formation and mutations at sites of class switching. *Nature* 414(6864):660-665.
9. Nagaoka H, Muramatsu M, Yamamura N, Kinoshita K, & Honjo T (2002) Activation-induced deaminase (AID)-directed hypermutation in the immunoglobulin Smu region: implication of AID involvement in a common step of class switch recombination and somatic hypermutation.

J Exp Med 195(4):529-534.

10. Catalan N*, et al.* (2003) The block in immunoglobulin class switch recombination caused by activation-induced cytidine deaminase deficiency occurs prior to the generation of DNA double strand breaks in switch mu region. *J Immunol* 171(5):2504-2509.
11. Barreto V, Reina-San-Martin B, Ramiro AR, McBride KM, & Nussenzweig MC (2003) C-terminal deletion of AID uncouples class switch recombination from somatic hypermutation and gene conversion. *Mol Cell* 12(2):501-508.
12. Ta VT*, et al.* (2003) AID mutant analyses indicate requirement for class-switch-specific cofactors. *Nat Immunol* 4(9):843-848.
13. Kotani A*, et al.* (2005) A target selection of somatic hypermutations is regulated similarly between T and B cells upon activation-induced cytidine deaminase expression. *Proc Natl Acad Sci U S A* 102(12):4506-4511.
14. Liu M*, et al.* (2008) Two levels of protection for the B cell genome during somatic hypermutation. *Nature* 451(7180):841-845.
15. Ramiro AR*, et al.* (2004) AID is required for c-myc/IgH chromosome translocations in vivo. *Cell* 118(4):431-438.
16. Kovalchuk AL*, et al.* (2007) AID-deficient Bcl-xL transgenic mice develop delayed atypical plasma cell tumors with unusual Ig/Myc chromosomal rearrangements. *J Exp Med* 204(12):2989-3001.
17. Epeldegui M, Hung YP, McQuay A, Ambinder RF, & Martinez-Maza O (2006) Infection of human B cells with Epstein-Barr virus results in the expression of somatic hypermutation-inducing molecules and in the accrual of oncogene mutations. *Mol Immunol*.
18. Matsumoto Y*, et al.* (2007) Helicobacter pylori infection triggers aberrant expression of activation-induced cytidine deaminase in gastric epithelium. *Nat Med* 13(4):470-476.

19. Endo Y, *et al.* (2007) Expression of activation-induced cytidine deaminase in human hepatocytes via NF-kappaB signaling. *Oncogene* 26(38):5587-5595.

20. Ishikawa C, Nakachi S, Senba M, Sugai M, & Mori N (2011) Activation of AID by human T-cell leukemia virus Tax oncoprotein and the possible role of its constitutive expression in ATL genesis. *Carcinogenesis* 32(1):110-119.

21. Lee CG, *et al.* (2001) Quantitative regulation of class switch recombination by switch region transcription. *J Exp Med* 194(3):365-374.

22. Bachl J, Carlson C, Gray-Schopfer V, Dessing M, & Olsson C (2001) Increased transcription levels induce higher mutation rates in a hypermutating cell line. *J Immunol* 166(8):5051-5057.

23. Aguilera A (2002) The connection between transcription and genomic instability. *Embo J* 21(3):195-201.

24. Lippert MJ, *et al.* (2011) Role for topoisomerase 1 in transcription-associated mutagenesis in yeast. *Proc Natl Acad Sci U S A* 108(2):698-703.

25. Takahashi T, Burguiere-Slezak G, Van der Kemp PA, & Boiteux S (2011) Topoisomerase 1 provokes the formation of short deletions in repeated sequences upon high transcription in Saccharomyces cerevisiae. *Proc Natl Acad Sci U S A* 108(2):692-697.

26. La Spada AR & Taylor JP (2010) Repeat expansion disease: progress and puzzles in disease pathogenesis. *Nat Rev Genet* 11(4):247-258.

27. Hubert L, Jr., Lin Y, Dion V, & Wilson JH (2011) Topoisomerase 1 and Single-Strand Break Repair Modulate Transcription-Induced CAG Repeat Contraction in Human Cells. *Mol. Cell. Biol.* 31(15):3105-3112.

28. Pommier Y (2006) Topoisomerase I inhibitors: camptothecins and beyond. *Nat Rev Cancer* 6(10):789-802.

29. Zhao J, Bacolla A, Wang G, & Vasquez KM (2010) Non-B DNA structure-induced genetic instability and evolution. *Cell Mol Life Sci* 67(1):43-62.

30. Miao ZH, *et al.* (2007) Nonclassic functions of human topoisomerase I: genome-wide and pharmacologic analyses. *Cancer Res* 67(18):8752-8761.

31. Tuduri S, *et al.* (2009) Topoisomerase I suppresses genomic instability by preventing interference between replication and transcription. *Nat Cell Biol* 11(11):1315-1324.

32. Kobayashi M, *et al.* (2009) AID-induced decrease in topoisomerase 1 induces DNA structural alteration and DNA cleavage for class switch recombination. *Proc Natl Acad Sci U S A* 106(52):22375-22380.

33. Faili A, *et al.* (2002) AID-dependent somatic hypermutation occurs as a DNA single-strand event in the BL2 cell line. *Nat Immunol* 3(9):815-821.

34. Urasaki Y, *et al.* (2001) Characterization of a novel topoisomerase I mutation from a camptothecin-resistant human prostate cancer cell line. *Cancer Res* 61(5):1964-1969.

35. Pourquier P, *et al.* (2002) Gemcitabine (2',2'-difluoro-2'-deoxycytidine), an antimetabolite that poisons topoisomerase I. *Clin Cancer Res* 8(8):2499-2504.

36. Bauer SR, Holmes KL, Morse HC, 3rd, & Potter M (1986) Clonal relationship of the lymphoblastic cell line P388 to the macrophage cell line P388D1 as evidenced by immunoglobulin gene rearrangements and expression of cell surface antigens. *J Immunol* 136(12):4695-4699.

37. Yoshikawa K, *et al.* (2002) AID enzyme-induced hypermutation in an actively transcribed gene in fibroblasts. *Science* 296(5575):2033-2036.

38. Morham SG, Kluckman KD, Voulomanos N, & Smithies O (1996) Targeted disruption of the mouse topoisomerase I gene by camptothecin selection. *Mol Cell Biol* 16(12):6804-6809.

39. Williams SK & Tyler JK (2007) Transcriptional regulation by chromatin disassembly and

reassembly. *Curr Opin Genet Dev* 17(2):88-93.

40. Drolet M*, et al.* (2003) The problem of hypernegative supercoiling and R-loop formation in transcription. *Front Biosci* 8:d210-221.

41. Liu LF & Wang JC (1987) Supercoiling of the DNA template during transcription. *Proc Natl Acad Sci U S A* 84(20):7024-7027.

42. Bacolla A & Wells RD (2004) Non-B DNA conformations, genomic rearrangements, and human disease. *J Biol Chem* 279(46):47411-47414.

43. Wells RD (2007) Non-B DNA conformations, mutagenesis and disease. *Trends Biochem Sci* 32(6):271-278.

44. Nicolas A (1998) Relationship between transcription and initiation of meiotic recombination: toward chromatin accessibility. *Proc Natl Acad Sci U S A* 95(1):87-89.

45. Blackwell TK*, et al.* (1986) Recombination between immunoglobulin variable region gene segments is enhanced by transcription. *Nature* 324(6097):585-589.

46. Gangloff S, Lieber MR, & Rothstein R (1994) Transcription, topoisomerases and recombination. *Experientia* 50(3):261-269.

47. Wright BE, Schmidt KH, Minnick MF, & Davis N (2008) I. VH gene transcription creates stabilized secondary structures for coordinated mutagenesis during somatic hypermutation. *Mol Immunol* 45(13):3589-3599.

48. Rogozin IB, Solovyov VV, & Kolchanov NA (1991) Somatic hypermutagenesis in immunoglobulin genes. I. Correlation between somatic mutations and repeats. Somatic mutation properties and clonal selection. *Biochim Biophys Acta* 1089(2):175-182.

49. Stanlie A, Aida M, Muramatsu M, Honjo T, & Begum NA (2010) Histone3 lysine4 trimethylation regulated by the facilitates chromatin transcription complex is critical for DNA cleavage in class switch recombination. *Proc Natl Acad Sci U S A* 107(51):22190-22195.

50. Borde V, *et al.* (2009) Histone H3 lysine 4 trimethylation marks meiotic recombination initiation sites. *Embo J* 28(2):99-111.

51. Matthews AG, *et al.* (2007) RAG2 PHD finger couples histone H3 lysine 4 trimethylation with V(D)J recombination. *Nature* 450(7172):1106-1110.

52. Doi T, Kinoshita K, Ikegawa M, Muramatsu M, & Honjo T (2003) De novo protein synthesis is required for the activation-induced cytidine deaminase function in class-switch recombination. *Proc Natl Acad Sci U S A* 100(5):2634-2638.

53. Mizushima S & Nagata S (1990) pEF-BOS, a powerful mammalian expression vector. *Nucleic Acids Res* 18(17):5322.

54. Oppezzo, P, *et al.* (2003) Chronic lymphocytic leukemia B cells expressing AID display dissociation between class switch recombination and somatic hypermutation. *Blood* 101(10):4029-4032.

55. Jolly CJ, Klix N & Neuberger MS (1997) Rapid methods for the analysis of immunoglobulin gene hypermutation: application to transgenic and gene targeted mice. 25(19): 1913-1919.

Figure Legends

Figure 1. Top1 reduction by AID activation, knockdown, and haploinsufficiency

(A) Top1 protein levels in BL2-AID$^{-/-}$AIDER cells in the presence of the indicated concentration of 4-oxyhydtroxy-tamoxifen (4-OHT) for the time intervals shown above. Western blots with anti-Top1 and anti-actin antibodies are shown below. Each sample was loaded in two lanes and the protein amount in the left lane is a half of that in the right lane. Top1/Actin, Top1 versus actin densitometry ratios relative to the 0 μM 4-OHT condition. **(B)** Efficiency of Top1 knockdown in BL2-AID$^{-/-}$AIDER cells. Whole-cell extracts were prepared 96 hr after introducing the indicated siRNA against Top1 or negative control oligos. **(C)** Scheme for generating the *Top1*^{f} and *Top1*$^{-}$ allele in the mouse *Top1* gene locus. Pgk-neo, PGK promoter-driven neomycin-resistance gene; DT-A, diphtheria toxin A; Probe A, Southern blot probe for genotyping; H, HindIII site. **(D)** Southern blot showing the *Top1*$^{f/+}$ allele and wild-type (*Top1*$^{+/+}$) genotypes. Tail DNA was digested with HindIII and probed with Probe A shown in **C**. **(E)** Top1 protein levels in spleen B cells from *Top1*$^{+/+}$ and heterozygote (*Top1*$^{-/+}$) littermates. Antibodies were the same as in **A**. The Top1/Actin ratios were normalized to the rightmost lane of *Top1*$^{+/+}$.

Figure 2. Top1 level inversely correlates with SHM frequency

(A) Western blot of Top1 (top panel), AIDER (2nd), GFP (3rd), and tubulin (lowest) proteins of parental P388 cells and their sublines, which include P388-AIDER, P388/CPT45-AIDER, and its stable transfectant with GFP or GFP-hTop1. Three different sizes of Top1 are indicated by arrows: arrow 1, endogenous Top1 (~100 kDa); arrow 2, P388/CPT45-specific Top1 (~135 kDa); arrow 3, GFP-hTop1 (~130 kDa); arrow 4, endogenous AID; arrow 5, AID-ER. Size marker positions are indicated at right. Triangle shows that two lanes of each sample have different protein amounts with the ratio of 2 to 3 on the left versus right lane. **(B)** Quantitative RT-PCR of the μ germinal transcripts

in P388 parental, P388/CPT45 subclones, and CH12 cells. **(C)** Proliferation curve of P388/CPT45-AIDER cells expressing the GFP (circle) or GFP-hTop1 (rectangle) protein.

Figure 3. SHM augmentation by Top1 knockdown depends on target transcription

(A) AIDER expression in NTZ-AIDER cells. The amount of protein loaded per lane was monitored using an anti-tubulin antibody. **(B)** Top1 protein levels after knockdown by the indicated siRNA oligos in NTZ-AIDER cells transfected with the indicated oligos and incubated for 24 hours. Cells were stimulated with 1 μM 4-OHT for a further 72 hours. Each sample was loaded in two lanes and the loaded protein amount in the left lane is a half of that in the right lane. **(C)** GFP reversion frequency after AIDER activation in Top1-knockdown cells and those transfected with control oligos. **(D)** GFP reversion frequency in a *tet* dilution series to decrease target transcription in Top1-knockdown NTZ-AIDER cells. The NTZ-AIDER cells were placed in different concentrations of *tet* on day 0, and transfected with siRNA oligos on day 1. 4-OHT was added on day 2, and SHM was evaluated on day 6.

Figure 4. Top1 inhibitor CPT suppresses SHM

(A) GFP reversion assay of NTZ-AIDER cells stimulated with 1 μM 4-OHT for 3 days in the presence or absence of 30 nM CPT. **(B)** Percentages of propidium iodide (PI)-negative live cells in the samples analyzed in **A**. **(C)** Quantification of GFP transcripts in the cell populations analyzed in **A.** The Q-PCR signals of GFP mRNA were normalized to the β-actin mRNA signal. **(D)** Western blots of the Top1 protein 3 hours after the activation of JP8BdelER in BL2 cells. Top1/actin, signal intensity ratio of Top1 versus actin protein. 4-OHT stimulated sample was loaded in two lanes, and the protein amount in the left lane is a half of that in the right lane.

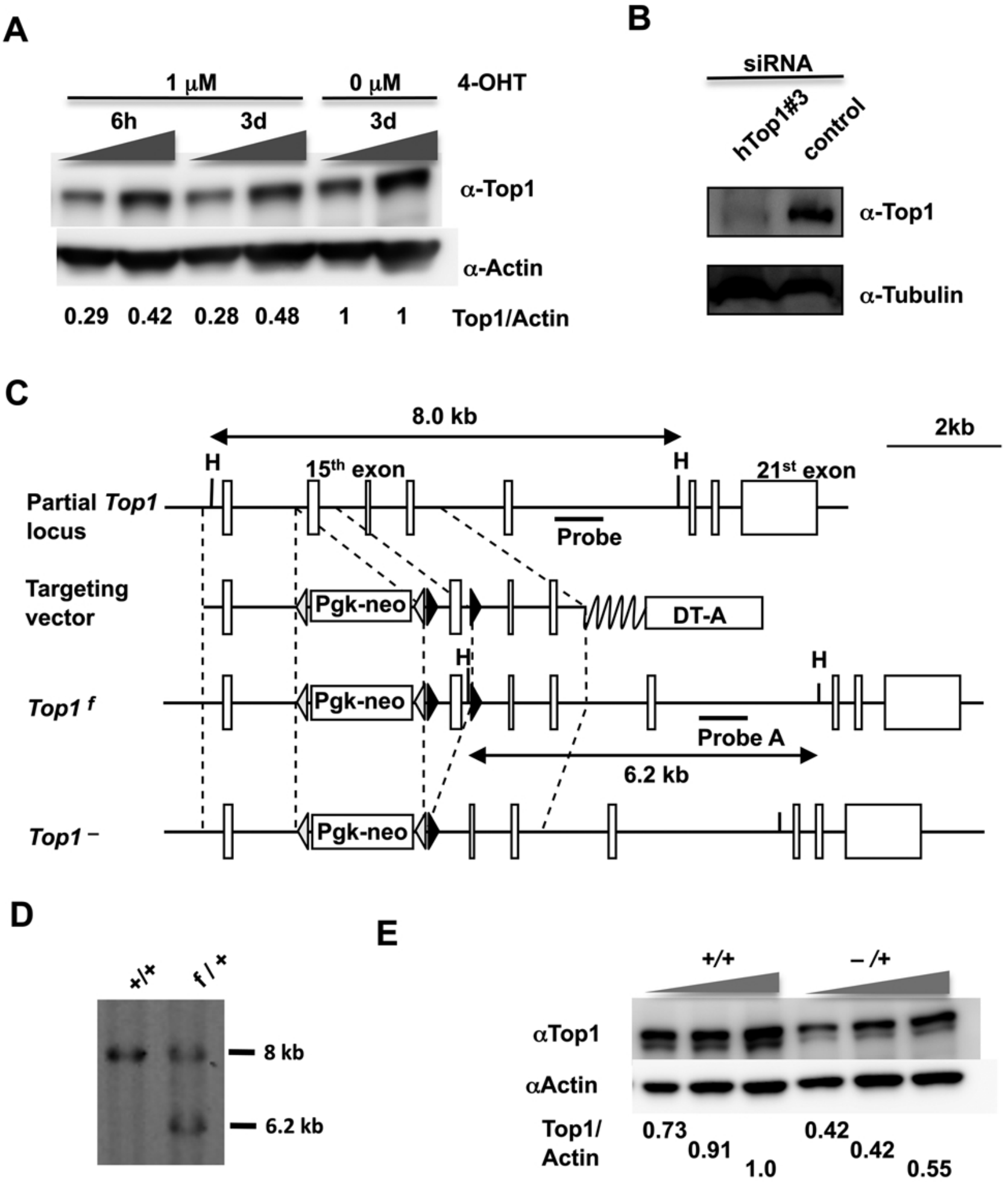
A
1 μM
0 μM
4-OHT
6h
3d
3d
α-Top1
α-Actin
0.29 0.42 0.28 0.48 1 1
Top1/Actin
B
siRNA
hTop1#3
control
α-Top1
α-Tubulin
C
8.0 kb
2kb
H
15th exon
H
21st exon
Partial Top1 locus
Probe
Targeting vector
Pgk-neo
DT-A
H
H
Top1 f
Pgk-neo
Probe A
6.2 kb
Top1 −
Pgk-neo
D
+/+
f/ x
8 kb
6.2 kb
E
+/+
– /+
αTop1
αActin
Top1/ Actin
0.73
0.91
1.0
0.42
0.42
0.55

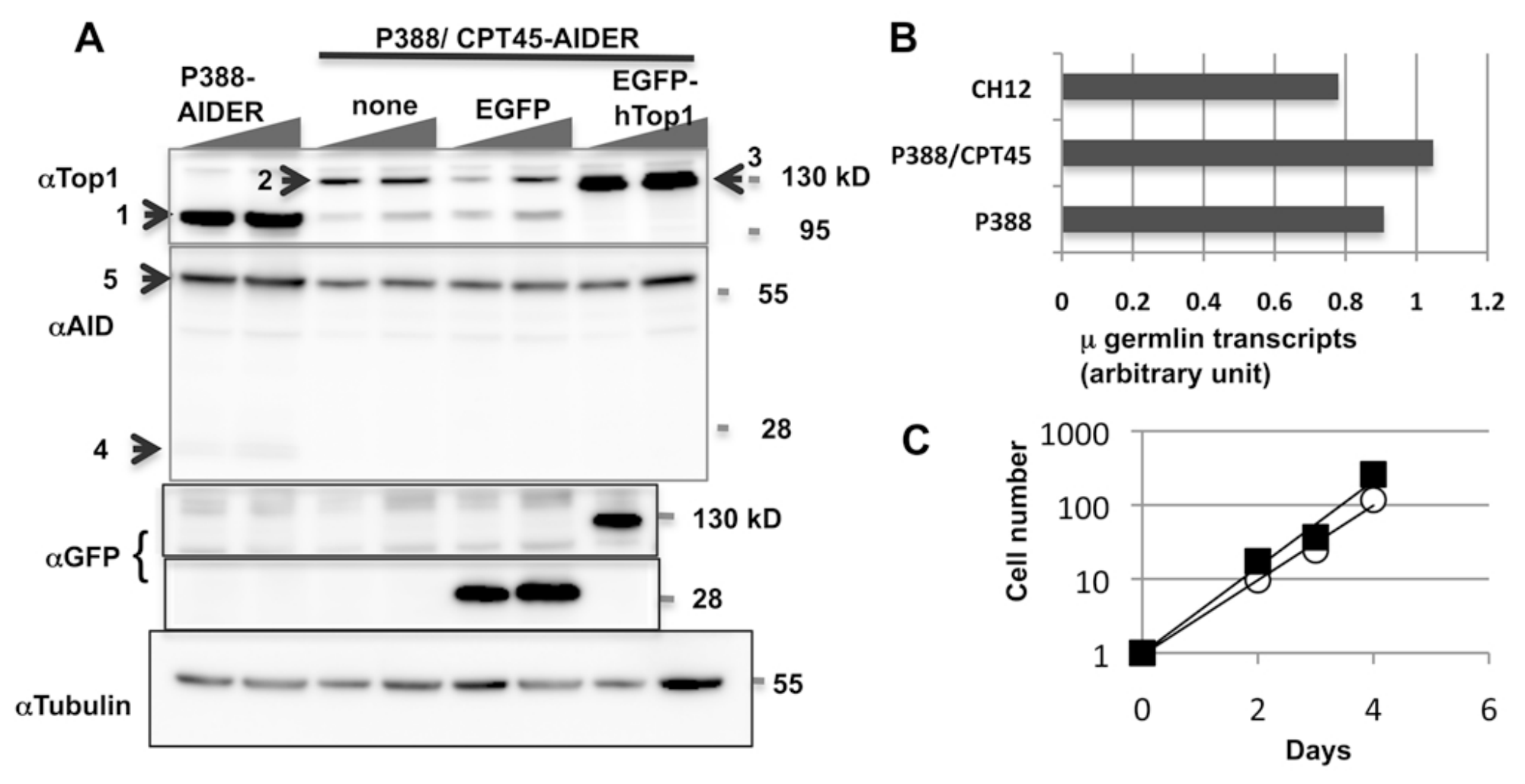
A
P388/ CPT45-AIDER
P388-AIDER
none
EGFP
EGFP-hTop1
αTop1
1
2
3
130 kD
95
5
αAID
55
4
28
αGFP
130 kD
28
αTubulin
55
B
CH12
P388/CPT45
P388
0
0.2
0.4
0.6
0.8
1
1.2
μ germlin transcripts (arbitrary unit)
C
Cell number
1000
100
10
1
0
2
4
6
Days

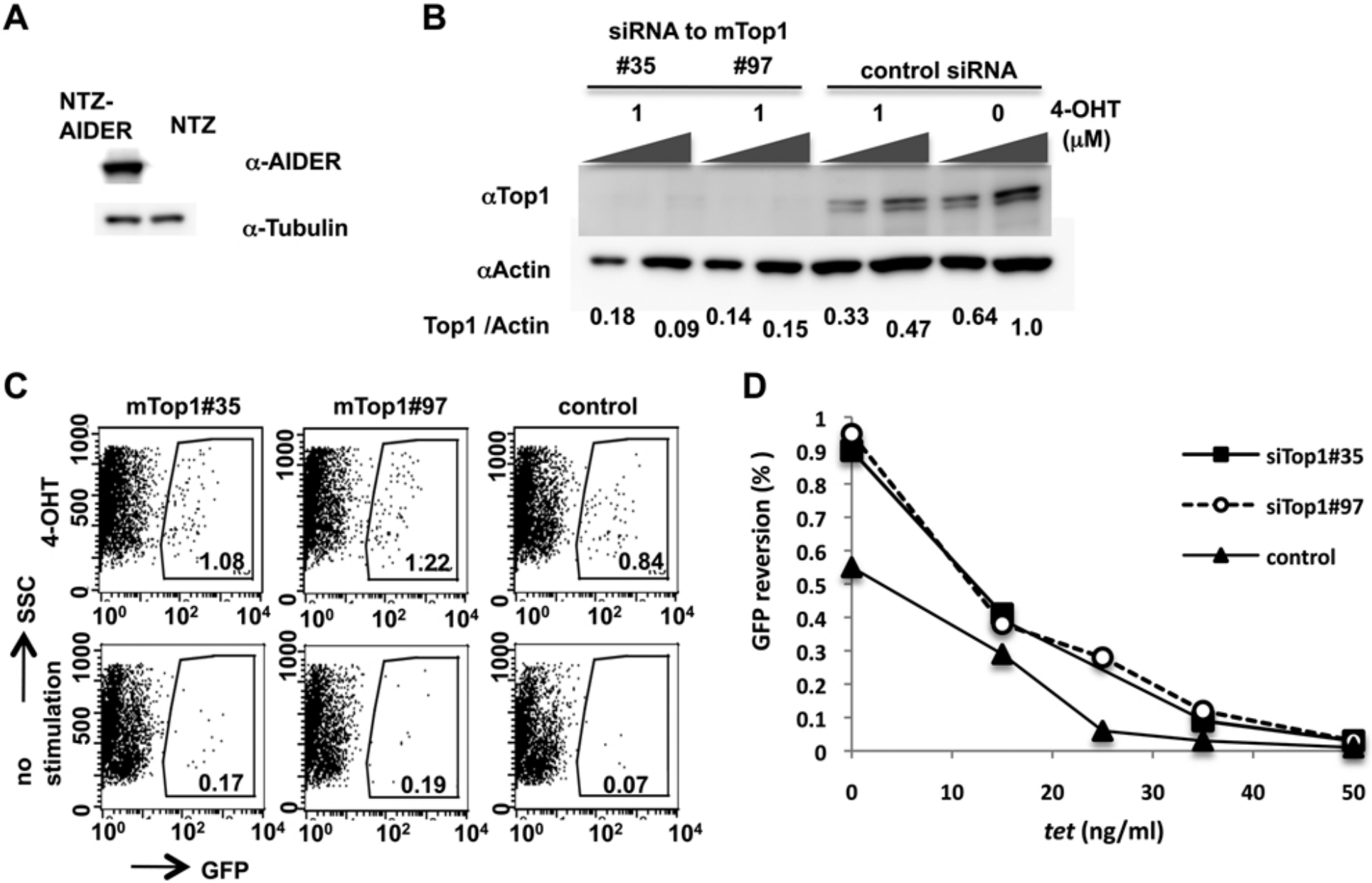
A
NTZ-AIDER
NTZ
α-AIDER
α-Tubulin
B
siRNA to mTop1
#35
#97
control siRNA
1
1
1
0
4-OHT (μM)
αTop1
αActin
Top1 /Actin
0.18
0.09
0.14
0.15
0.33
0.47
0.64
1.0
C
mTop1#35
mTop1#97
control
4-OHT
no stimulation
SSC
GFP
1.08
1.22
0.84
0.17
0.19
0.07
D
GFP reversion (%)
tet (ng/ml)
siTop1#35
siTop1#97
control

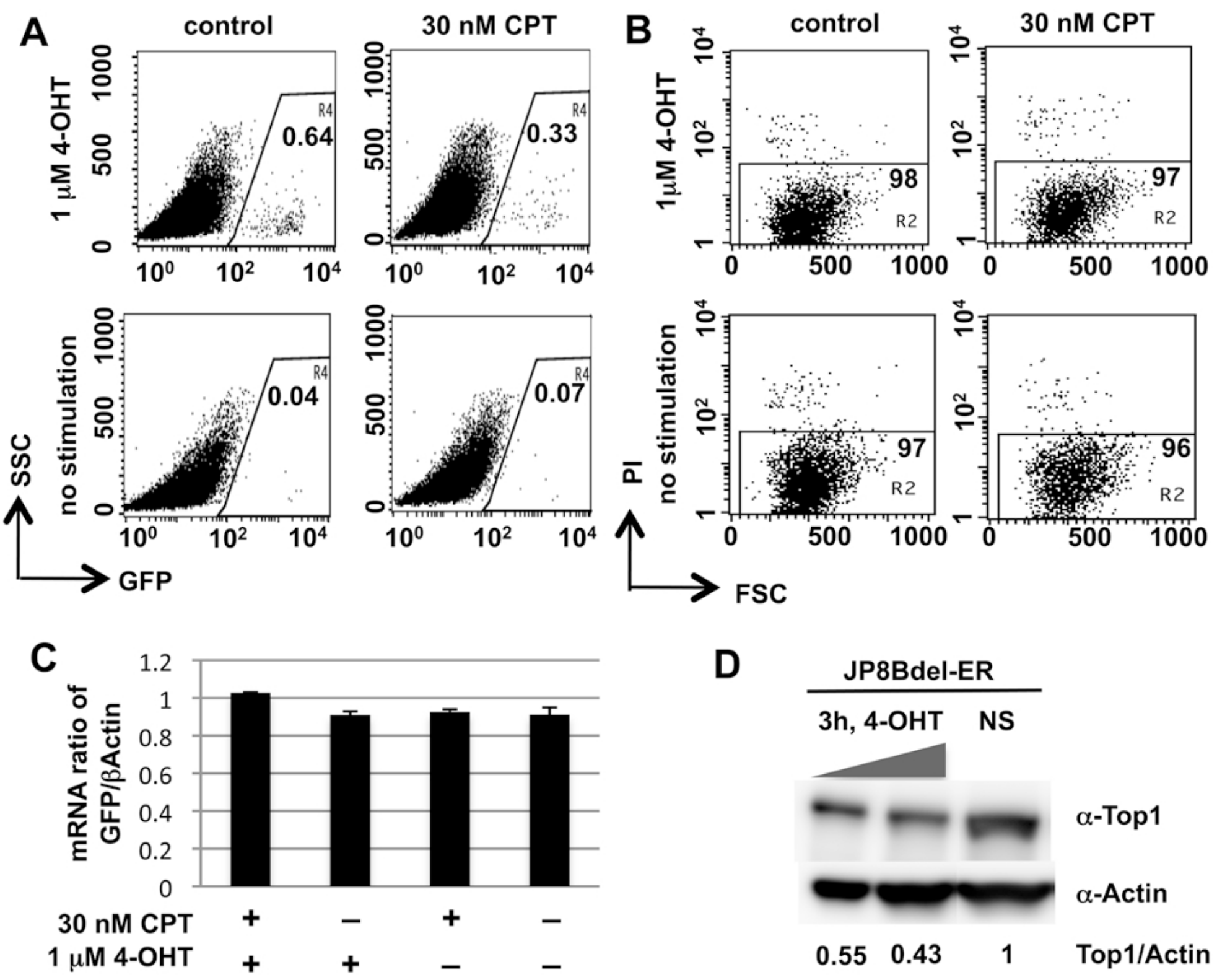
A
control
30 nM CPT
1 μM 4-OHT
no stimulation
R4
0.64
0.33
0.04
0.07
SSC
GFP
B
control
30 nM CPT
1μM 4-OHT
no stimulation
98
97
97
96
R2
PI
FSC
C
mRNA ratio of GFP/βActin
1.2
1
0.8
0.6
0.4
0.2
0
30 nM CPT + – + –
1 μM 4-OHT + + – –
D
JP8Bdel-ER
3h, 4-OHT
NS
α-Top1
α-Actin
0.55 0.43 1
Top1/Actin

Table 1. SHM frequency in the V and Sμ regions in BL2-AID$^{-/-}$AIDER cells and germinal center B cells

4-OHT (nM)	siRNA	Mutated /clones	Mutation rate ($\times 10^{-4}$) (mutated/total bases)	
A. 100	hTop1#3	18 / 189	2.7[a]	(21 / 78,624)
	control	13 / 197	1.6[b]	(13 / 81,952)
0	hTop1#3	2 / 126	0.4[c]	(2 / 52,416)
	control	3 / 140	0.5[d]	(3 / 58,240)
B. 100	hTop1#3	27 / 69	5.3[e]	(59 / 112,263)
	control	28 / 74	3.5[f]	(42 / 120,398)
0	hTop1#3	6 / 42	1.0[g]	(7 / 68,334)
	control	6 / 35	1.2[h]	(7 / 56,945)
C. Litter (wks)	genotype *Top1*			
#1 (20)	+/–	34 / 75	125[i]	(467 / 37,500)
	+/+	22 / 69	44[j]	(152 / 34,000)
#2 (16)	+/–	22 / 23	317[k]	(365 / 11,500)
	+/+	14 / 23	131[l]	(165 / 11,500)
#3 (25)	+/–	31 / 44	219[m]	(482 / 22,000)
	+/+	6 / 17	93[n]	(79 / 8,500)
	+/+	7 / 12	126[o]	(76 / 6,000)

A, B. BL2 AID$^{-/-}$ AIDER cells were incubated for 3 days with 4-OHT. The 416-bp-long re-arranged V_H4-39-J_H5 region (33) and the 5' end of the Sμ core region cloned by hSμ-A and hSμ-D (1,627 bp) (54) were sequenced, in **A** and **B**, respectively. **C**. Germinal center B cells from Peyer's patches of Top1 heterozygote and wild-type littermates were recovered. The 500-bp 3' end of the J_H4 region (55) was analyzed. Deletion and insertion numbers are shown in Table S3-S6 and not counted in the mutation rates throughout the present study. *p*-value by Fisher's exact test: a vs. b, 9.3×10^{-2}; b vs. c, 4×10^{-5}; b vs. d, 5.1×10^{-2}; e vs. f, 3×10^{-2}; e vs. g, 7×10^{-7}; f vs. h, 3.8×10^{-3}; i vs. j, 2.5×10^{-32}; k vs. l, 4.4×10^{-19}; m vs. n, 3.2×10^{-15} ; m vs. o, 1.2×10^{-6}

Table 2. SHM in the Sμ region in P388 cells

Cells	4-OHT (μM)	Mutated /clones	Mutation rate ($\times 10^{-4}$) (mutated/total bases)	
A. P388- AIDER	1	11 / 143	0.71[a]	(11 / 155,012)
	0	4 / 154	0.36	(6 / 166,936)
P388/CPT45	1	31 / 144	2.56[b]	(39 / 156,096)
-AIDER	0	4 / 149	0.25[c]	(4 / 161,516)
B. P388/CPT45 -AIDER with GFP	1	24 / 89	6.3[d]	(35 / 55,981)
	0	2 / 93	0.5[e]	(3 / 58,497)
P388/CPT45 -AIDER with GFP-hTop1	1	9 / 81	2.2[f]	(11 / 50,949)
	0	4 / 92	0.7[g]	(4 / 57,868)

A. P388-AIDER and P388/CPT45-AIDER cells were stimulated with 4-OHT for 7 days. The 1,084-bp Iμ/Sμ region (9) amplified by mSμA-mSμD was sequenced. **B.** Cells were stimulated as in A. The 629-bp segment between mSμB-mSμD was analyzed. *p*-value by Fisher's exact test: a vs. b, 5×10^{-5}; b vs c, 8.4×10^{-9}; d vs. f, 8×10^{-4}; d vs. e, 1.6×10^{-8}; f vs. g, 0.03

Table 3. SHM of an artificial construct in NTZ cells

4-OHT (μM)	siRNA	Mutated /clones	Mutation rate ($\times 10^{-3}$) (mutated/total bases)
1	mTop1#35	23 / 28	4.5[a] (111 / 24,836)
	mTop1#97	28 / 30	4.7[b] (124 / 26,610)
	control	24 / 29	2.9[c] (76 / 25,723)
0	mTop1#35	3 / 31	0.11[d] (3 / 27,497)
	mTop1#97	6 / 30	0.23[e] (6 / 26,610)
	control	1 / 31	0.04[f] (1 / 27,497)

NTZ cells transfected with siRNA oligos were incubated with 4-OHT for 3 days. The GFP region was sequenced (37). *p*-value by Fisher's exact test: a vs. c, 3×10^{-3}; b vs. c, 4×10^{-4}; a vs. d, 3×10^{-32}; b vs. e, 3×10^{-31} ; c vs. f, 3.8×10^{-23}; d vs. f, 0.3; e vs. f, 0.057

Table 4. CPT effects on SHM frequency

4-OHT (μM)	CPT (nM)	Mutated /clones	Mutation rate ($\times 10^{-4}$) (mutated/total bases)	
A. 0	0	7 / 83	0.95	(7 / 73,621)
1	0	26 / 84	6.1[a]	(46 / 74,508)
0	30	1 / 88	0.13[b]	(1 / 78,056)
1	30	12 / 90	1.5[c]	(12 / 79,830)
B. 0	0	6 / 54	1.7	(8 / 46,008)
1	0	33 / 81	7.2[d]	(50 / 69,012)
1	30	22 / 98	3.5[e]	(29 / 83,496)

A. Genomic DNA was recovered from NTZ-AIDER cells exposed to 30 nM CPT for 3 days together with 4-OHT, and the *GFP* gene was sequenced (37).

B. BL2-JP8BdelER cells were exposed to 30 nM CPT for 25 hours together with 4-OHT for the last 24 hours. The 5' region of Sμ amplified with hSμ-B and hSμ-D (852 bp) was sequenced. *p*-value by Fisher's exact test; a vs. c, 1.2×10^{-6}; b vs. c, 1.9×10^{-3}; d vs. e, 9.5×10^{-4}